

**Supplementary Information for:
Selective sensing of ethylene and glucose using
carbon-nanotube-based sensors: An ab initio
investigation**

Yan Li^{*a}, Miroslav Hodak^a, Wenchang Lu^{a,b}, and J. Bernholc^{*a,b}

^aCenter for High Performance Simulation and Department of Physics, North Carolina State University, Raleigh, NC 27695-7518, USA

^bComputer Science and Mathematics Division, Oak Ridge National Laboratory, Oak Ridge, TN 37831, USA

*E-mail addresses: *yli26@ncsu.edu* (Y. Li), *bernholc@ncsu.edu* (J. Bernholc)

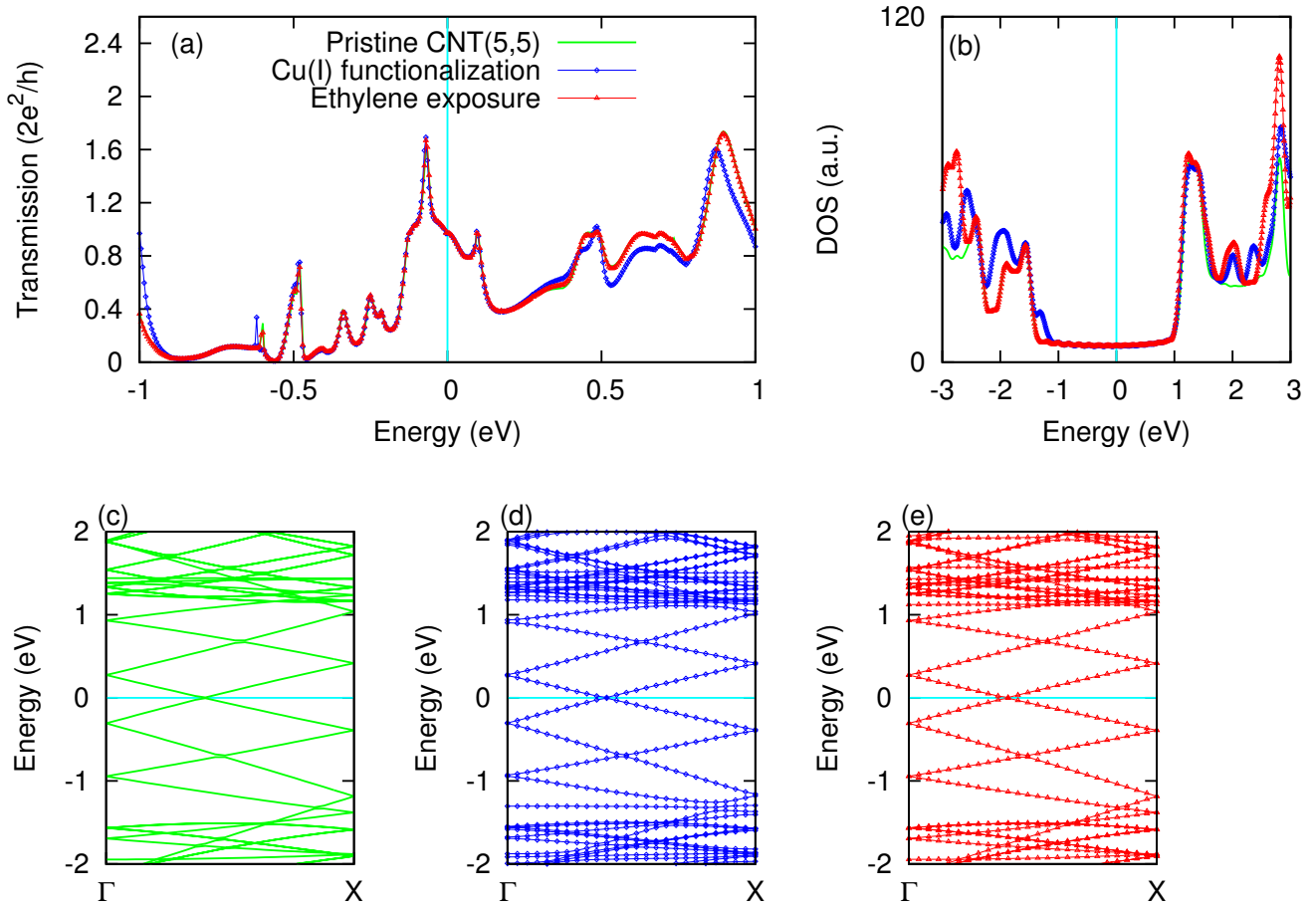


Figure 1S: (a) Transmission spectra of the metallic (5,5) CNT-based sensor for ethylene detection at 100 mV source-drain bias. (b) Total density of states (DOS) of the metallic (5,5) CNT-based sensor at different stages of ethylene detection, and (c)-(e) corresponding band structures. Note that the gold electrodes are not included in the density of states and band structure calculations. The Fermi level is shifted to zero and indicated by the cyan line in all the plots.

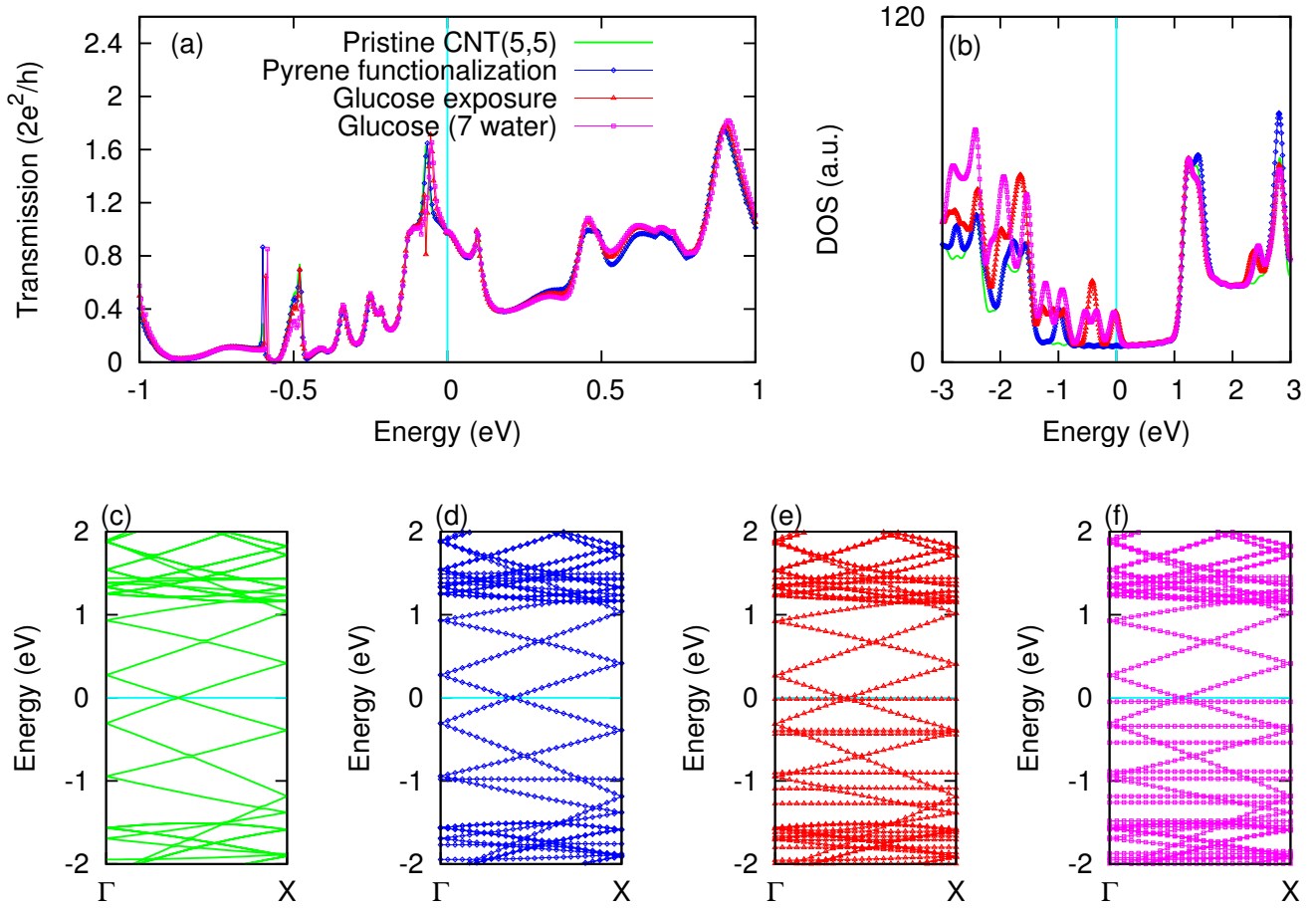


Figure 2S: (a) Transmission spectra of the metallic (5,5) CNT-based sensor for glucose detection at 100 mV source-drain bias. (b) Total density of states (DOS) of the metallic (5,5) CNT-based sensor at different stages of glucose detection, and (c)-(f) corresponding band structures. Note that the gold electrodes are not included in the density of states and band structure calculations. The Fermi level is shifted to zero and indicated by the cyan line in all the plots.

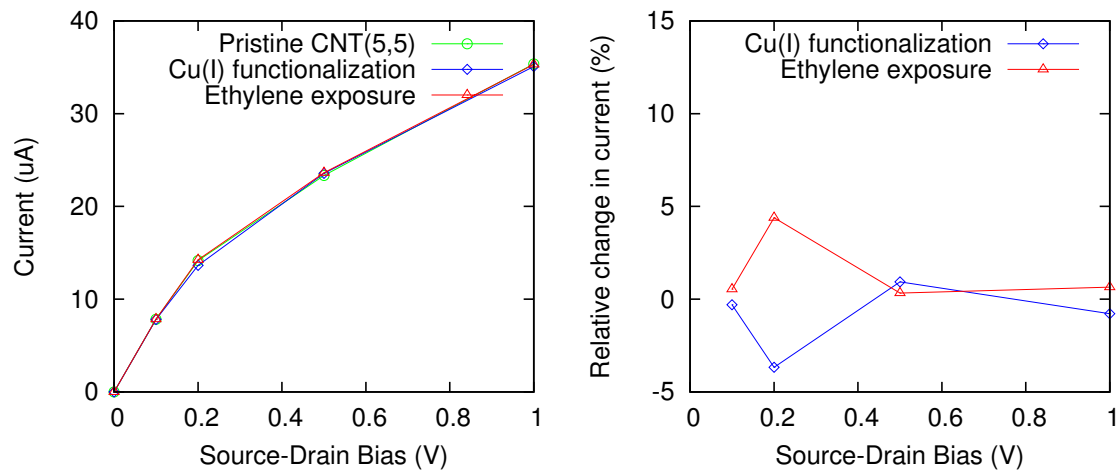


Figure 3S: I-V curves (left) of ethylene detection using the metallic (5,5) CNT-based sensor device, and the relative changes of electrical currents (right) with respect to the previous step.

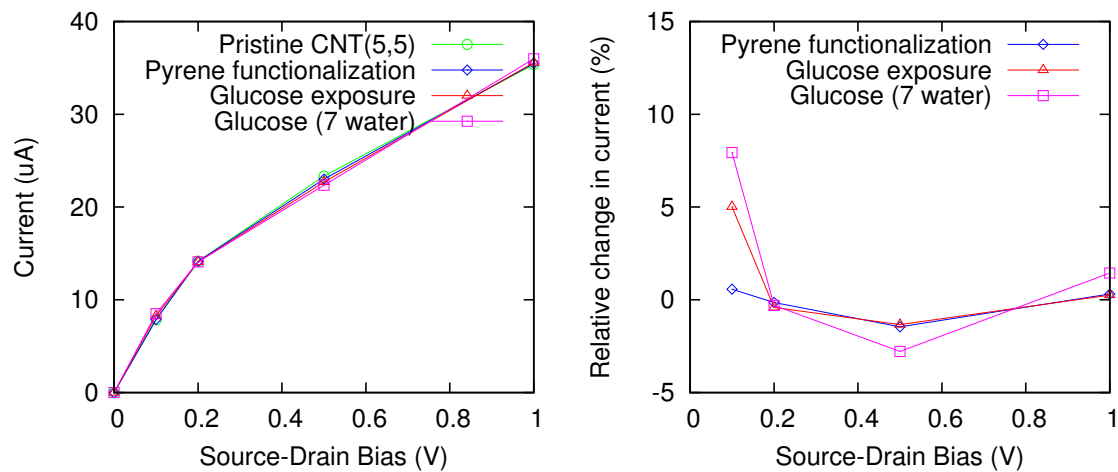


Figure 4S: I-V curves (left) of glucose detection using the metallic (5,5) CNT-based sensor device, and the relative changes of electrical currents (right) with respect to the previous step.

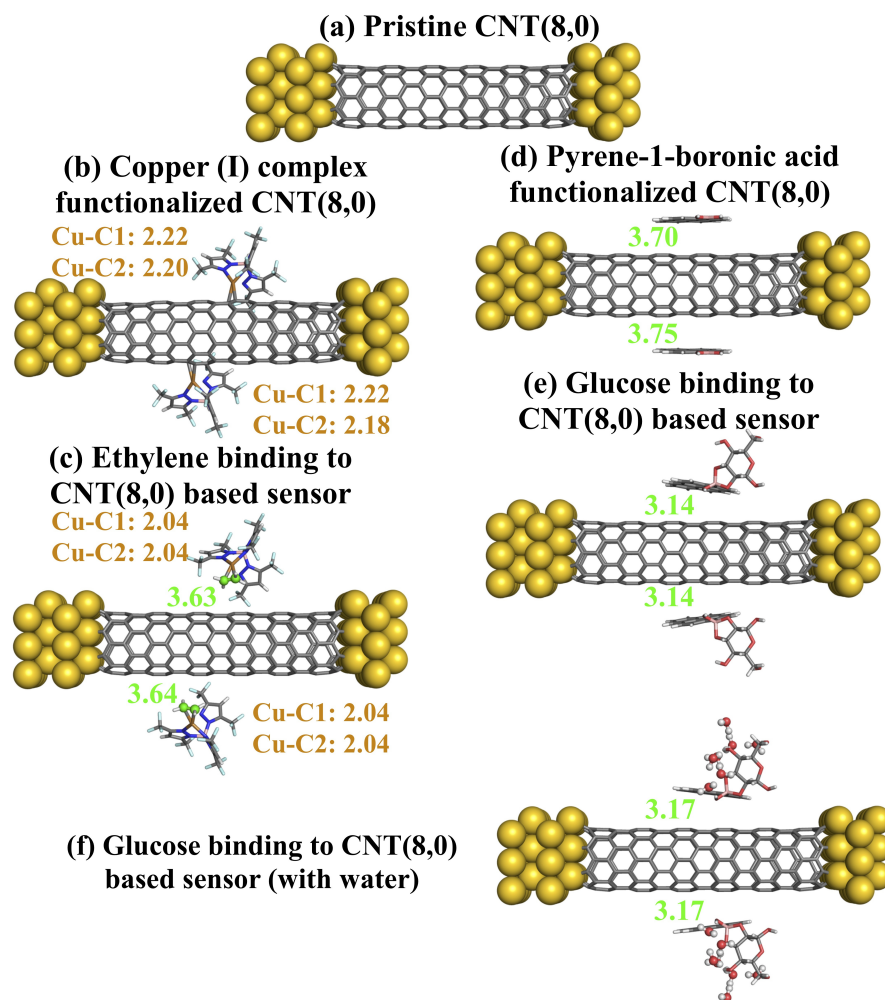


Figure 5S: Optimized structures of two functionalized receptor molecules for ethylene detection (a, b, c) and glucose detection (a, d, e, f) in semiconducting CNT(8,0)-based systems. The colors of Au, C, N, O, H, F, Cu, B are gold, grey, blue, red, white, cyan, brown and pink, respectively. The ethylene molecules are displayed in the ball-and-stick representation with their carbon atoms shown in green. The copper-carbon bond lengths (in Å) are labeled in brown; the closest distances between the ethylene molecule and the nanotube surface (in Å) are labeled in green. Similarly, the closest distances between the pyrene-1-boronic acid molecule and the nanotube surface (in Å) are labeled in green. The 7 water molecules near glucose are displayed in the ball-and-stick representation.

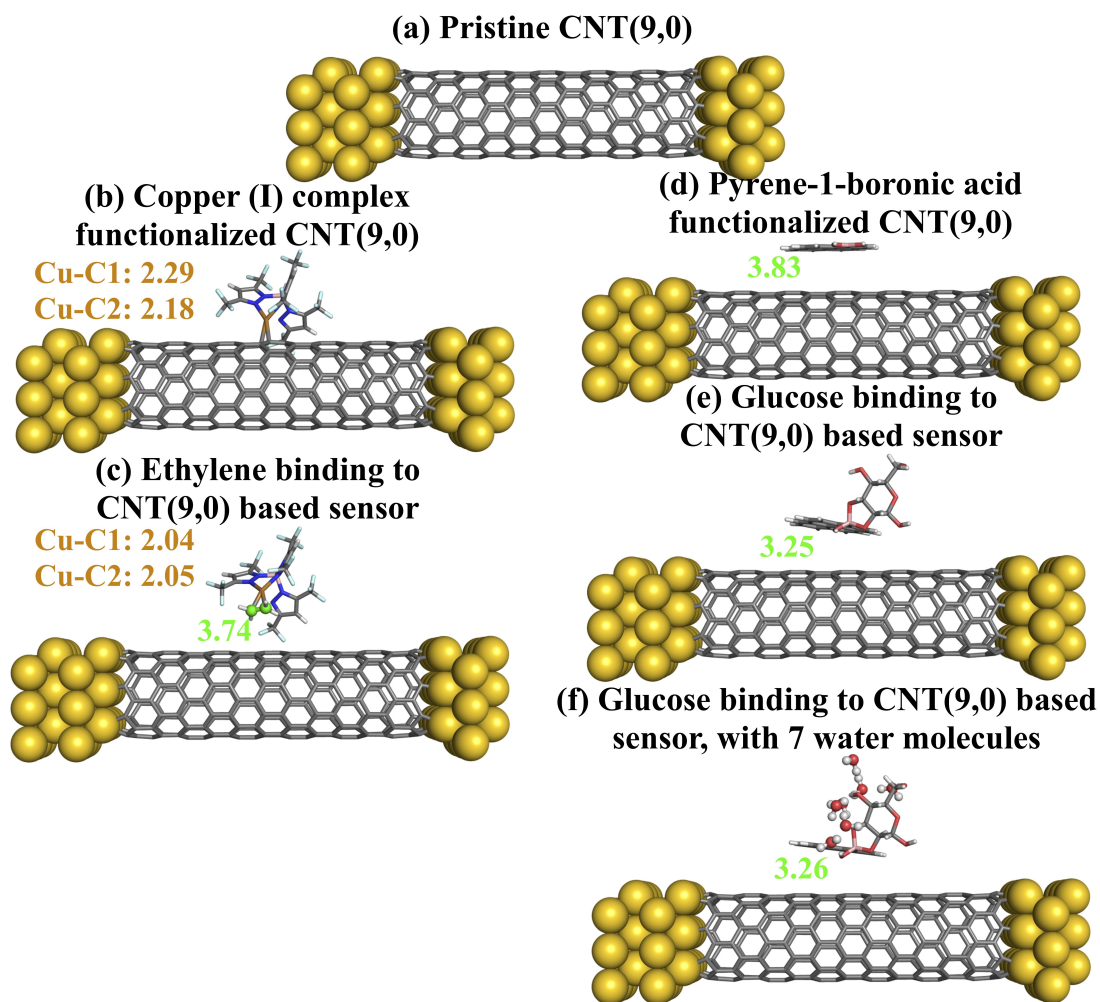


Figure 6S: Optimized structures for ethylene detection (a, b, c) and glucose detection (a, d, e, f) in semiconducting CNT(9,0)-based systems. The colors of Au, C, N, O, H, F, Cu, B are gold, grey, blue, red, white, cyan, brown and pink, respectively. The ethylene molecules are displayed in the ball-and-stick representation with their carbon atoms shown in green. The copper-carbon bond lengths (in Å) are labeled in brown; the closest distances between the ethylene molecule and the nanotube surface (in Å) are labeled in green. Similarly, the closest distances between the pyrene-1-boronic acid molecule and the nanotube surface (in Å) are labeled in green. The 7 water molecules near glucose are displayed in the ball-and-stick representation.

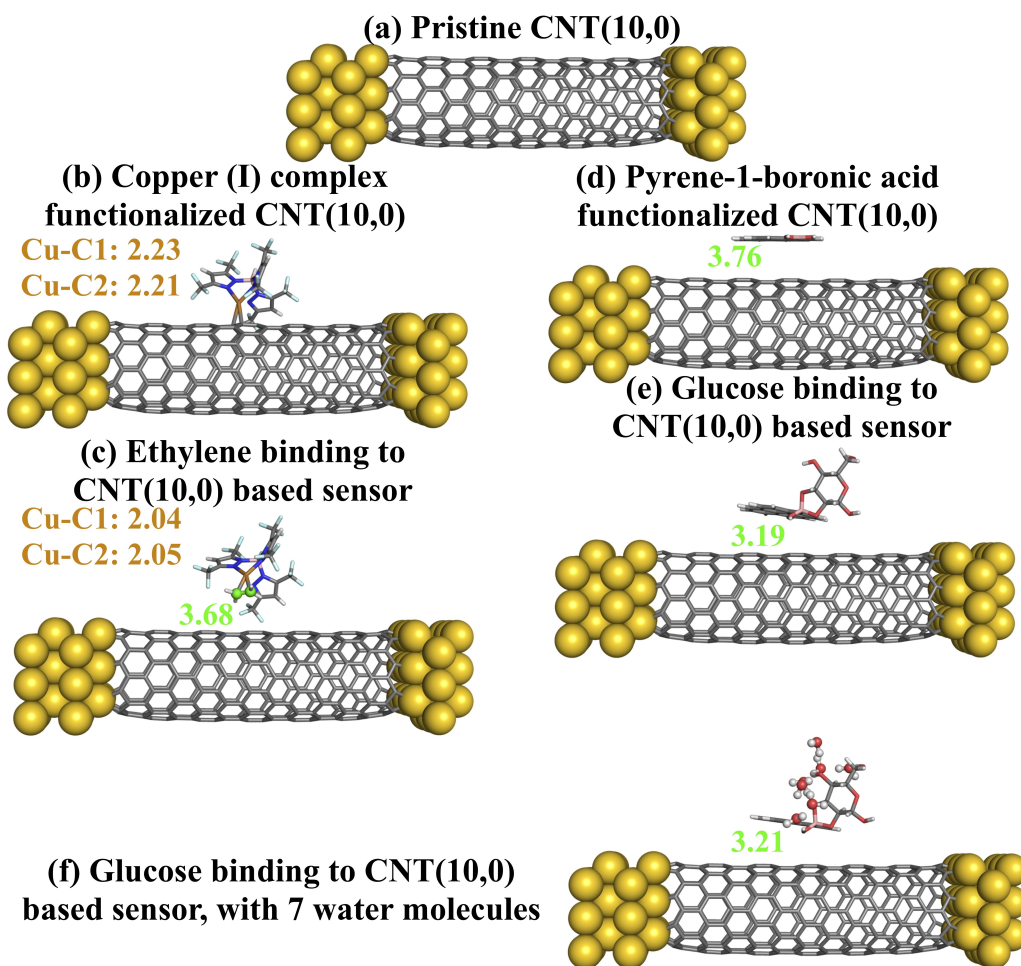


Figure 7S: Optimized structures for ethylene detection (a, b, c) and glucose detection (a, d, e, f) in semiconducting CNT(10,0)-based systems. The colors of Au, C, N, O, H, F, Cu, B are gold, grey, blue, red, white, cyan, brown and pink, respectively. The ethylene molecules are displayed in the ball-and-stick representation with their carbon atoms shown in green. The copper-carbon bond lengths (in Å) are labeled in brown; the closest distances between the ethylene molecule and the nanotube surface (in Å) are labeled in green. Similarly, the closest distances between the pyrene-1-boronic acid molecule and the nanotube surface (in Å) are labeled in green. The 7 water molecules near glucose are displayed in the ball-and-stick representation.

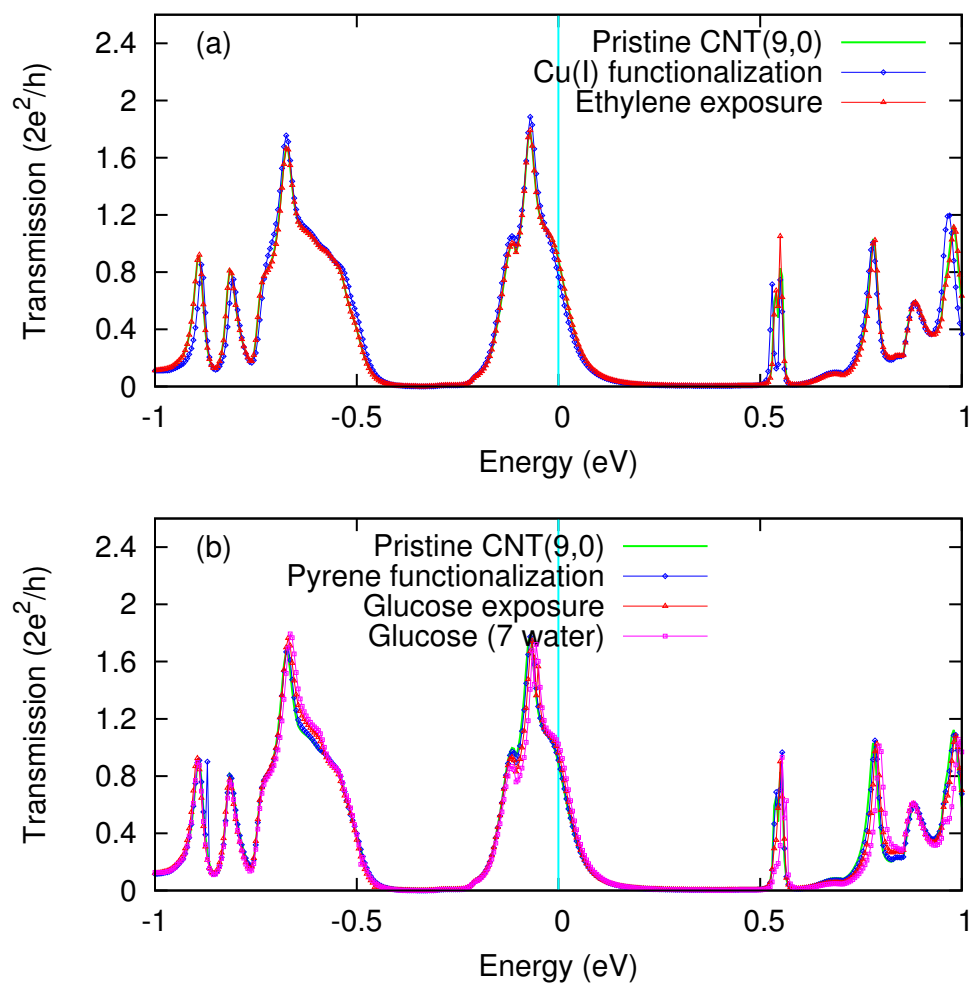


Figure 8S: Transmission spectra at 100 mV of the semiconducting (9,0) nanotube for (a) ethylene and (b) glucose detection, respectively. The Fermi level is shifted to zero and indicated by the cyan line.

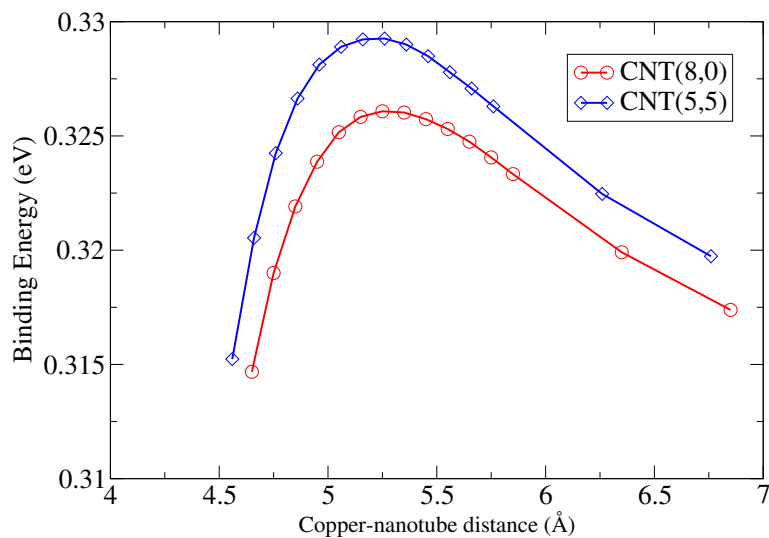


Figure 9S: Binding energy between the ethylene-bound copper(I) complex and CNT versus the copper-nanotube distance, calculated using the PBE functional. The red line with circles represents the semiconducting CNT(8,0)-based sensor devices, where the maximum of the curve corresponds to the optimized structure in Fig. 1(c) in the paper; the blue line with diamonds represents the metallic CNT(5,5)-based sensor device, where the maximum of the curve corresponds to the optimized structure in Fig. 1(f) in the paper. When van der Waals interactions are included via the vdW-DF functional, the binding energy at the maximum of the curve increases to 0.94 eV in (8,0) CNT and 0.98 eV in (5,5) CNT.